Resources, Conservation & Recycling

The effect of temperature and concentration of urine sludge on rheological characterization

--Manuscript Draft--

Manuscript Number:	
Article Type:	Full Length Article
Keywords:	Urine pipeline; Urine sludge; Precipitation; Rheological parameter; Rheological models
Corresponding Author:	Zifu Li, Ph.D. University of Science and Technology Beijing Beijing, CHINA
First Author:	Zhengxu Yan
Order of Authors:	Zhengxu Yan
	Zifu Li, Ph.D.
	Shikun Cheng
	Jian Zhang
	Devendra P Saroj
	Yanzhao Han
	Lingling Zhang
	Lei Zheng
	Mingxiang Xue
Abstract:	The formation of phosphorus-based solids in urine diversion systems, which results in the pipe blockage is the main challenge for large-scale implementation of urine source separation. The gravitational sedimentation leads to a large solid concentration gradient in the horizontal pipelines, which results in the variability in the urine sludge (consisting of human urine and sediment) rheological characteristics. This study aimed to provide the accurate rheological data of urine sludge to improve the design of the urine transportation pipe systems, and explained the influence of urine sludge non-Newtonian characteristic on pipe blockage. In this work, the rheograms of urine sludge were obtained using a narrow gap rotating rheometer. Origin 2021 software (based on the least square method) and genetic algorithm were used to obtain the rheometric data fits. The results showed that urine sludge behaved like Newtonian fluid at low concentrations. As concentration increased, urine sludge presented a shear thinning behavior, which could be described using the Herschel–Bulkley model. An Arrhenius-type equation was used to describe the temperature effect on sludge viscosity. The effect of concentration on the rheological behavior of urine sludge reflected on the rheological model parameters. The limiting viscosity, yield stress, and consistency index increased with urine sludge concentration increase, which were represented using an empirical exponential model, power law, and exponential model, respectively. The behavior index n decreased with concentration increase, which was described using a linear model. The results may provide the fundamental support for better understanding the hydraulic characteristics and blockage problems of urine.
Suggested Reviewers:	Dana Komínková kominkovad@fzp.czu.cz
	Joachim Behrendt j.behrendt@tuhh.de
	Chad Staddon Chad.Staddon@uwe.ac.uk

The effect of temperature and concentration of urine sludge on rheological characterization

Zhengxu Yan[a], Zifu Li[a,*], Shikun Cheng[a,*], Jian Zhang[b], Devendra P. Saroj[c], Yanzhao Han[a], Lingling Zhang[a], Lei Zheng[a], Mingxiang Xue[d]

[a] *School of Energy and Environmental Engineering, Beijing Key Laboratory of Resource-oriented Treatment of Industrial Pollutants, University of Science and Technology Beijing, Beijing 100083, PR China*

[b] *EnviroSystems Engineering & Technology Co., Ltd., Tiangong Plaza A501, Xueyuan Road 30, Haidian District, Beijing, 100083, PR China*

[c] *Centre for Environmental Health Engineering (CEHE), Department of Civil and Environmental Engineering, Faculty of Engineering and Physical Sciences, University of Surrey, Surrey GU2 7XH, United Kingdom*

[d] *Beijing Jiaotong University*

** Corresponding author*

E-mail addresses: zifulee@aliyun.com, chengshikun@ustb.edu.cn

Tel: +86-010-62334378; Fax: +86-010-62334378

Abstract

The formation of phosphorus-based solids in urine diversion systems, which results in the pipe blockage is the main challenge for large-scale implementation of urine source separation. The gravitational sedimentation leads to a large solid concentration gradient in the horizontal pipelines, which results in the variability in the urine sludge (consisting of human urine and sediment) rheological characteristics. This study aimed to provide the accurate rheological data of urine sludge to improve the design of the urine transportation pipe systems, and explained the influence of urine sludge non-Newtonian characteristic on pipe blockage. In this work, the rheograms of urine sludge were obtained using a narrow gap rotating rheometer. Origin 2021 software (based on the least square method) and genetic algorithm were used to obtain the rheometric data fits. The results showed that urine sludge behaved like Newtonian fluid at low concentrations. As concentration increased, urine sludge presented a shear thinning behavior, which could be described using the Herschel–Bulkley model. An Arrhenius-type equation was used to describe the temperature effect on sludge viscosity. The effect of concentration on the rheological behavior of urine sludge reflected on the rheological model parameters. The limiting viscosity, yield stress, and consistency index increased with urine sludge concentration increase, which were represented using an empirical exponential model, power law, and exponential model, respectively. The behavior index n decreased with concentration increase, which was described using a linear model. The results may provide the fundamental support for better understanding the hydraulic characteristics and blockage problems of urine.

Key words: Urine pipeline; Urine sludge; Precipitation; Rheological parameter; Rheological models;

1. Introduction

Considering that current urban water management (UWM) strategies are not enough to address challenges such as rapidly aging infrastructure, population growth, and increasing urbanization, alternative solutions to conventional UWM are required (Tove et al., 2016). Urine source separation has been proposed to be the potential sustainable solutions for nutrient recovery, water conservation, pharmaceutical sequestration, and environmental performance (Boyer and Saetta, 2019). However, microbial ureolysis occurs in the urine diversion systems, which rapidly leads to an increased pH with the subsequent precipitation of struvite (MAP), hydroxyapatite (HAP), and calcite, which is advantageous for phosphorus recovery but can also block the pipe systems (Udert et al., 2003; Udert et al., 2003a, b).

Although significant advancements have been made in controlling urine precipitation in the urine diversion systems (Christiaens et al., 2019; Hellström et al., 1999; Randall et al., 2016; Saetta et al., 2019), the design and operation optimization aspects of the urine transported pipe systems, bridging source and treatment facilities, have been neglected. The main reason for this negligence is that most sanitation projects of urine source separation avoided the use of expensive separate pipelines and treated urine on-site or transported to a centralized treatment plant by truck (Chipako and Randall, 2020; Kavvada et al., 2017). However, rapid urbanization is concentrating urine source in urban areas. For dense urban settings, rental space required, rent, human labor, electricity, and transportation logistics may become barriers to the large-scale implementation of decentralized urine treatment techniques (Chipako and Randall, 2020; Kavvada et al., 2017). Moreover, an increased population density, which results in the low per capita costs for the construction and operation of the separate urine pipelines (Dodane et al., 2012), may prompt the decision makers to establish separate pipes for urine collection. For the further development of urine source separation, the transport systems in urine diversion require comprehensive assessment.

The design and optimization of the transportation systems for urine diversion require good knowledge with regard to transported liquid rheology. In the urine diversion systems, settleable solids accumulate at the bottom of the horizontal pipe section leading to large concentration gradients of suspended solids in urine fluid. Eshtiaghi et al. (2012) found that a slight increase in sludge concentration caused a steep increase in the transition velocity from turbulent to laminar flow. Accurate prediction of the transition velocity is important because ignoring the non-Newtonian character of the fluid could result in blockage in pipes when the fluid behavior changed from turbulent to laminar flow (Eshtiaghi et al., 2012). Sludge behaved like Newtonian fluid when diluted and became non-Newtonian with the increase of solid concentration (Thiène et al., 2019). The description of the rheological behavior of non-Newtonian sludge typically required two or three rheological parameters rather than a single viscosity value, which made designing of the pumping systems a complicated task because engineers required accurate rheological data instead of relying on the rule-of-thumb approaches (Farno et al., 2018).

Although many studies have been conducted on the rheological characterization of municipal sludge (Eshtiaghi et al., 2013; Ratkovich et al., 2013; Seyssiecq et al., 2003), little information is available regarding the rheological behavior of urine sludge. Therefore, this study aimed to investigate the basic characteristics of the rheological behavior of urine sludge and provide important parameter data to improve the design of the urine transported pipe systems. In this work, the rheograms obtained from experimental rheological measurements had been used to build viscosity models. The effect of concentration and temperature on the rheological behavior of urine sludge was investigated through correlating the rheological parameters with concentrations and temperatures. The effect of the variability in the urine sludge rheological characteristics on the design and optimization of piping systems is discussed.

2. Method and material

2.1. Urine sludge sample preparation

Real urine was collected from the storage tank installed at the urinal in an office building, at the University of Science and Technology Beijing, China. The collected urine was stored in a plastic tank at room temperature for several days. Microbial ureolysis rapidly led to an increased pH with the subsequent precipitation of calcium and magnesium mineral compounds during storage of urine (Udert et al., 2003b). The particle-size distribution of precipitates in urine sludge (Figure 1) was analyzed with a Mastersizer 3000 (Malvern Instruments Ltd., Worcestershire, United Kingdom) to calculate the minimum gap size (the results were the average of three analyses).

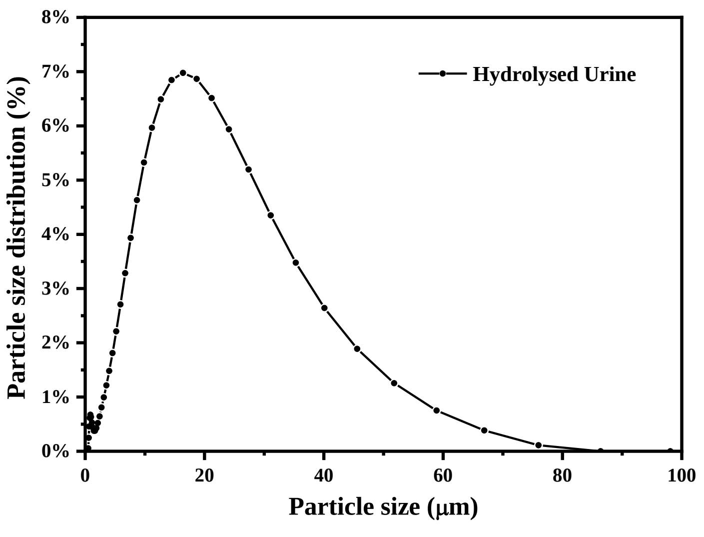

Figure 1. particle size distribution of urine sludge

The samples were concentrated by centrifugation at 6000 rpm (3700 G), and then the concentrated samples were diluted using the supernatant to prepare various concentrations of urine sludge samples. Total suspended solid (TSS, wt./wt.) was determined gravimetrically by drying samples to constant mass at 23 °C. In addition, the supernatant filtered through 0.45 μm syringe filters was used as a sample with 0% TSS. All the samples were homogenized before any rheological measurement. A summary of the various concentrations used for rheology is presented in Table 1.

Table 1 A summary of the various concentration samples

Sample ID	TSS (%)
1	0
2	1.3
3	3.2
4	5.3
5	8.5
6	11.2
7	11.8

2.2. Rheological measurements

Rotational rheometers equipped with concentric cylinder (CC) geometry have become widely accepted rheometer used in sludge rheology (Eshtiaghi et al., 2013). Rheological measurements were performed with an MCR302 instrument from Anton Paar (Graz, Austria) equipped with a CC system (Figure 2). The annular gap should be larger than the largest particles of the sample and should be small to minimize the correction factors and avoid turbulences (Seyssiecq et al., 2003). The minimum gap size should be 10 times as large as the representative particle size of the samples (Thota Radhakrishnan et al., 2018). Particle-size distribution (Figure 1) was used to calculate the minimum gap size. The particle-size range in the sample was 0–76 μm. Therefore, this geometry had an annular gap size of 1151.5 μm, achieving the minimum gap size (760 μm). Rheology was measured at 10 °C, 20 °C, 30 °C, and 40 °C for each concentration to determine the impact of temperature on the rheological behavior. A Peltier temperature control system was used to control the temperature with an accuracy of ±0.1 °C. The sample was covered with a lid installed on the cup to avoid evaporation. For each measurement, the sample was pre-sheared for 5 min at a shear rate of 1000 s^{-1} and remained stable for 5 min to erase material memory and ensure reproducible results (Thota Radhakrishnan et al., 2018; Wang et al., 2016). There is no accurate indication of the transition between laminar and turbulent regimes for the rotational rheometers equipped with concentric cylinders (Seyssiecq et al., 2003). When the inner cylinder exceeded a critical rotational speed, a transition to the Taylor flow or onset of turbulence could occur, which caused an overestimation of the measured torque (Thota Radhakrishnan et al., 2015). The shear rate range was determined to avoid the overestimation of torque at high shear rates (Thota Radhakrishnan et al., 2015).

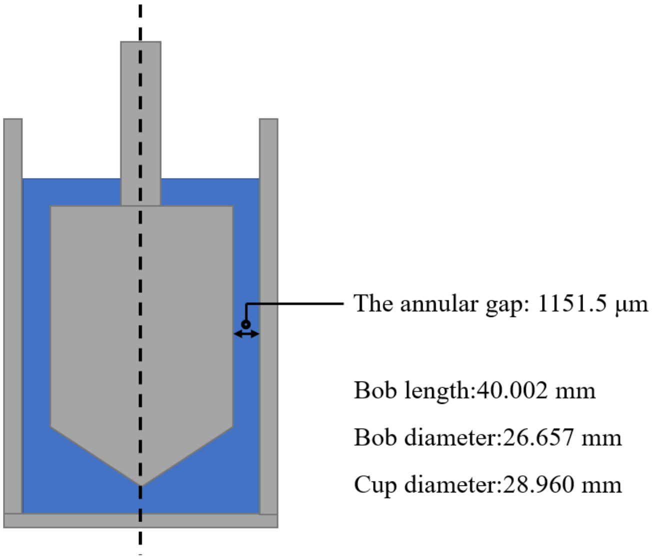

Figure 2. Schematic diagram of concentric cylinder (CC)

2.3. Rheological model

Municipal sludge is composed of water, mineral particles, and organic matter (Baudez et al., 2013), which is similar to urine sludge. This work gained knowledge from previous research experiences of the rheological behavior of municipal sludge. Most of the rheological models were the results of experiments, which were used to describe the graphical representation of shear stress versus shear rate (Thota Radhakrishnan et al., 2018). The rheological information on sludge obtained from the test carried out over a range of shear stresses or shear rates was often extrapolated by several orders of magnitude to predict the behavior of sludge at the high-shear region (turbulent regime) (Eshtiaghi et al., 2013). Therefore, selecting the rheological model was important for modeling experimental data. The rheological models commonly used to describe sludge behavior are presented in Table 2 (Eshtiaghi et al., 2013; Seyssiecq et al., 2003).

Table 2. The rheological models. τ is the shear stress (Pa), $\dot{r}$ is the shear rate (1/s), K is the flow

consistency index (Pa·s^n), τ_0 is the yield stress (Pa), n is the flow behavior index.

$\tau = K\dot{r}$	the Newtonian model	Equation 1
$\tau = K\dot{r}^n$	the Ostwald model	Equation 2
$\tau = \tau_0 + K\dot{r}$	the Bingham model	Equation 3
$\tau = \tau_0 + K\dot{r}^n$	the Herschel-Bulkley (HB) model	Equation 4

In selecting the appropriate rheological model, researchers were always guided by performance indicators such as R-squared and root-mean-square-error (RMSE) values, which systematically indicated the models with more parameters (more parameters would create more degrees of freedom to fit functions to experimental data) (Ratkovich et al., 2013). However, over-parameterization would over fit the data rather than represent the true underlying relation. Thota Radhakrishnan et al., (2018) found that when determining the appropriate model for low TSS content domestic sludge, although RMSE values indicated the Bingham model fits better, a linear model was chosen as the yield stress from the Bingham model was < 0.01 Pa. Hence, in selecting appropriate models, in addition to the necessary data fitting, researchers should check the procedure used to derive models thoroughly (Ratkovich et al., 2013). In this work, Origin 2021 software (based on the least square method) and genetic algorithm (presented in figure 3) were used to obtain the rheometric data fits. The adjusted R-Square was used to assess the predictive capability of the rheological models fitted by using Origin 2021 software. RMSE was calculated to obtain the fitness value and select the optimal solution when using genetic algorithm. More information on genetic algorithm could be found in the literature (Rooki et al., 2012; Thota Radhakrishnan et al., 2018).

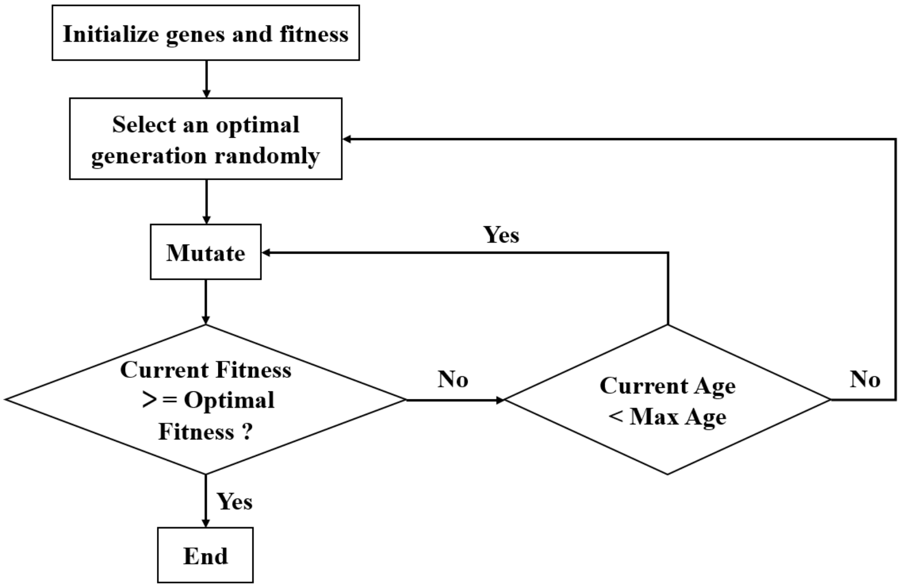

Figure 3. Flowchart of genetic algorithm procedure.

3. Results and discussions

3.1. Rheological modeling

It seems straightforward to perform data fitting (to obtain a fitting function suitable for the experimental data) through these algorithms. However, modelers often overlook the quality of the numbers obtained from algorithms (Ratkovich et al., 2013). The danger of overfitting and over-parameterization is discussed in section 2.3, and further information on the critical considerations of good modeling practice can be found in Ratkovich et al. (2013).

In this work, the rheometric data in steady-state laminar flow for urine sludge at various concentrations and temperatures were obtained using the rheological measurement approach mentioned in section 2.2. The rheometric data fitting results obtained by using Origin 2021 software and genetic algorithm were shown in Table A1 and Table A2. The results obtained from the two different algorithms were similar. Based on the adjusted R-Square and RMSE values from the parameter estimations, the best model was selected to describe the relationships between shear stress and shear rate. When TSS concentrations ≥ 5.3%, a significant non-linear/non-Newtonian relationship was observed. The adjusted R-Square and RMSE values indicated the HB model. Notably, at 40 ℃ and TSS concentrations of 5.3%, the relationship between the shear stress and shear rate was between linear and nonlinear. The adjusted R-Square value and RMSE value indicated the Bingham and HB models, respectively. At TSS concentrations of 3.2 %, although the RMSE values indicated that HB model fitted better at various temperature, Bingham model which was chosen as the shear thinning behavior was observed for concentrated sludge (Thota Radhakrishnan et al., 2018). Similar results were observed when using the adjusted R-Square value at 20 ℃ and TSS concentrations of 3.2%. Moreover, the yield stress τ_0 was not a measured quantity and was obtained from the rheometric data as a model parameter. Although the adjusted R-Square value indicated that the yield stress τ_0 was not observed at 10 °C and 40 ℃ and TSS concentrations of 3.2%, other results seemed to imply that the yield stress τ_0 existed and was > 0.01 Pa (the minimum threshold yield stress) (Thota Radhakrishnan et al., 2018). Therefore, the Bingham model might be suitable to describe the rheogram at TSS concentrations of 3.2%. At TSS concentrations ≤ 1.3%, the adjusted R-Square value indicated the Newtonian model, which implied that a significant linear relationship was observed at low %TSS. The RMSE value indicated that the Ostwald model fitted better at TSS concentrations of 1.3%, 10 °C and 30 ℃, which might be caused by the increase in the degree of freedom for optimization by adding another parameter. In addition, the estimation of model parameters was dependent on the choice of objective function, model structure, and solver. There is no perfect algorithm for estimating nonlinear model parameters. Furthermore, the rheometric data always contained random errors (Farno et al., 2018)

In this work, the Newtonian model was selected to fit the rheometric data obtained at TSS concentrations ≤ 1.3%, and the parameters for the Newtonian model were obtained from the results of using Origin 2021 software based on the least square method. At TSS concentrations of 3.2%, the Bingham model was selected to fit the rheometric data, and the parameters were obtained from the results of using genetic algorithm as this algorithm provided reasonable results in the fitting of the yield stress. At TSS concentrations ≥ 5.3%, the HB model fitted better. Although the estimated parameters for the HB model obtained from Origin 2021 software and genetic algorithm were similar, the results from genetic algorithm were selected as it could provide better solutions on non-linear fitting optimization in comparison with other methods (Rooki et al., 2012; Thota Radhakrishnan et al., 2018). Table 3 shows the final estimated parameters and the respective models used for fitting to describe the rheograms. The rheometric data in steady-state laminar flow were used to create the rheograms for urine sludge at various concentrations and temperatures, which are shown in Figure 4.

Table 3 The parameters for respective models describing the rheograms of urine sludge

Concentration	Temperature	Model	τ_0	K	n
% TSS	℃	-	Pa	Pa·s^n	-
0	10	Newtonian	0	0.00169	1
	20	Newtonian	0	0.00133	1
	30	Newtonian	0	0.001	1
	40	Newtonian	0	0.000970983	1

1.3	10	Newtonian	0	0.00202	1
	20	Newtonian	0	0.00156	1
	30	Newtonian	0	0.00122	1
	40	Newtonian	0	0.00103	1
3.2	10	Bingham	0.02956931	0.00324227	1
	20	Bingham	0.02614734	0.00258134	1
	30	Bingham	0.0300288	0.00214429	1
	40	Bingham	0.02699365	0.00178117	1
5.3	10	HB	0.10269181	0.00987139	0.89845639
	20	HB	0.09871291	0.00722623	0.91227097
	30	HB	0.10278852	0.00574912	0.91558099
	40	HB	0.10449259	0.00367615	0.96468986
8.5	10	HB	0.41181163	0.03013344	0.80466496
	20	HB	0.39780332	0.02129677	0.82117114
	30	HB	0.4039104	0.01515505	0.84103684
	40	HB	0.362537	0.01355263	0.82838114
11.2	10	HB	0.76935175	0.10226952	0.69353407
	20	HB	0.79531973	0.05241087	0.74072189
	30	HB	0.83717267	0.04194303	0.74402257
	40	HB	0.79906866	0.03435327	0.74580198
11.8	10	HB	0.81330176	0.11408465	0.68144895
	20	HB	0.86605676	0.05832704	0.72987134

	30	HB	0.8604639	0.05141247	0.72007678
	40	HB	0.83611631	0.04237313	0.72273118

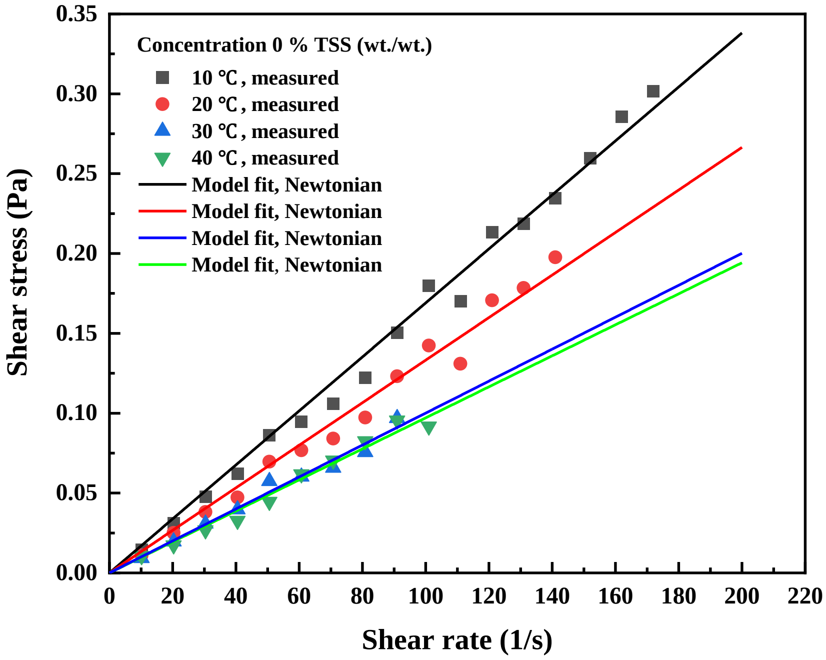

(a)

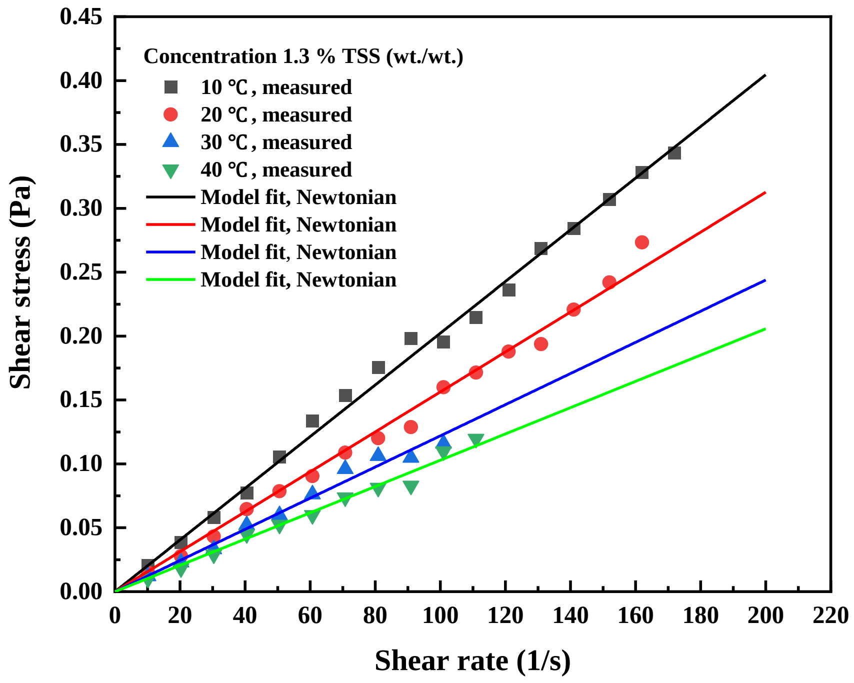
Concentration 1.3 % TSS (wt./wt.)
10 ℃, measured
20 ℃, measured
30 ℃, measured
40 ℃, measured
Model fit, Newtonian
Model fit, Newtonian
Model fit, Newtonian
Model fit, Newtonian
Shear stress (Pa)
Shear rate (1/s)

(b)

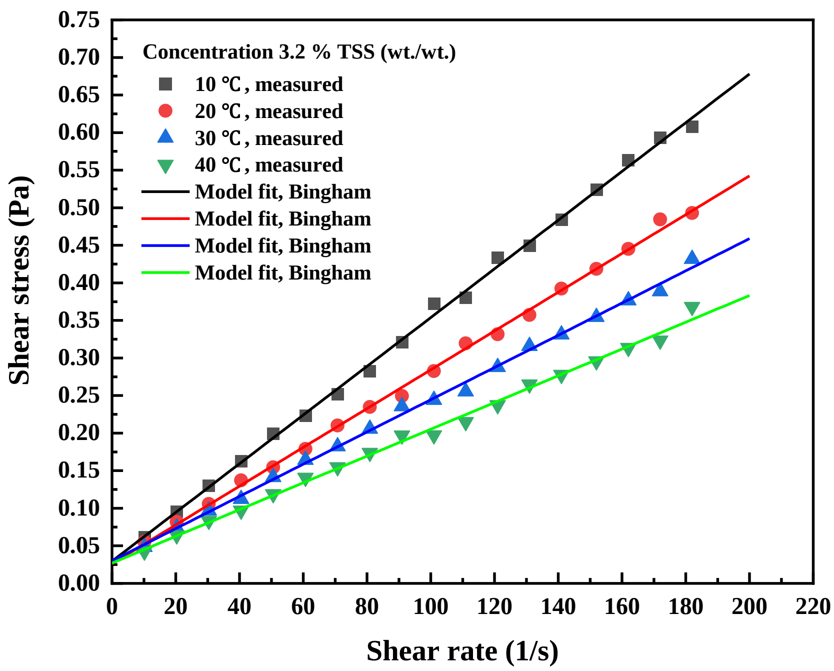
Concentration 3.2 % TSS (wt./wt.)
10 ℃, measured
20 ℃, measured
30 ℃, measured
40 ℃, measured
Model fit, Bingham
Model fit, Bingham
Model fit, Bingham
Model fit, Bingham
Shear stress (Pa)
Shear rate (1/s)

(c)

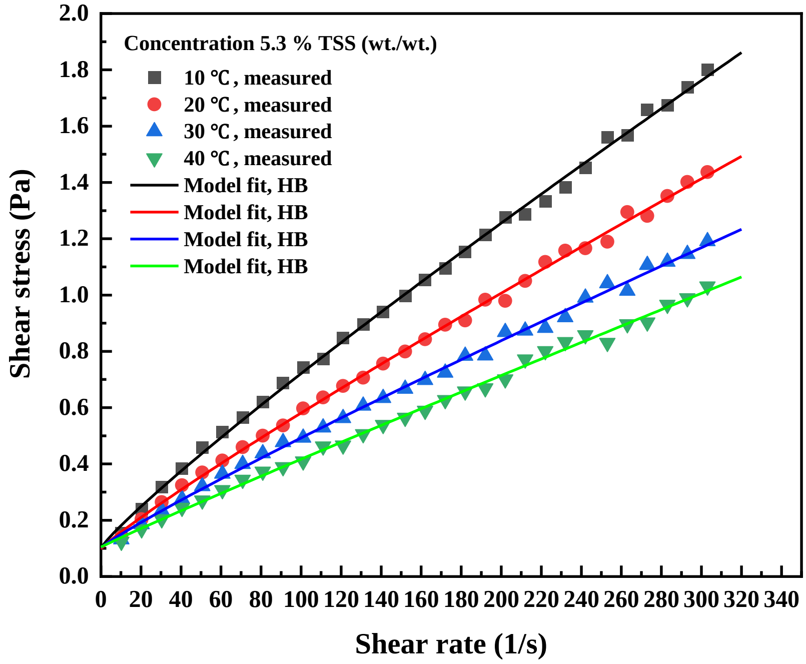
Concentration 5.3 % TSS (wt./wt.)
10 ℃, measured
20 ℃, measured
30 ℃, measured
40 ℃, measured
Model fit, HB
Model fit, HB
Model fit, HB
Model fit, HB
Shear stress (Pa)
Shear rate (1/s)
0.0
0.2
0.4
0.6
0.8
1.0
1.2
1.4
1.6
1.8
2.0
0 20 40 60 80 100 120 140 160 180 200 220 240 260 280 300 320 340

(d)

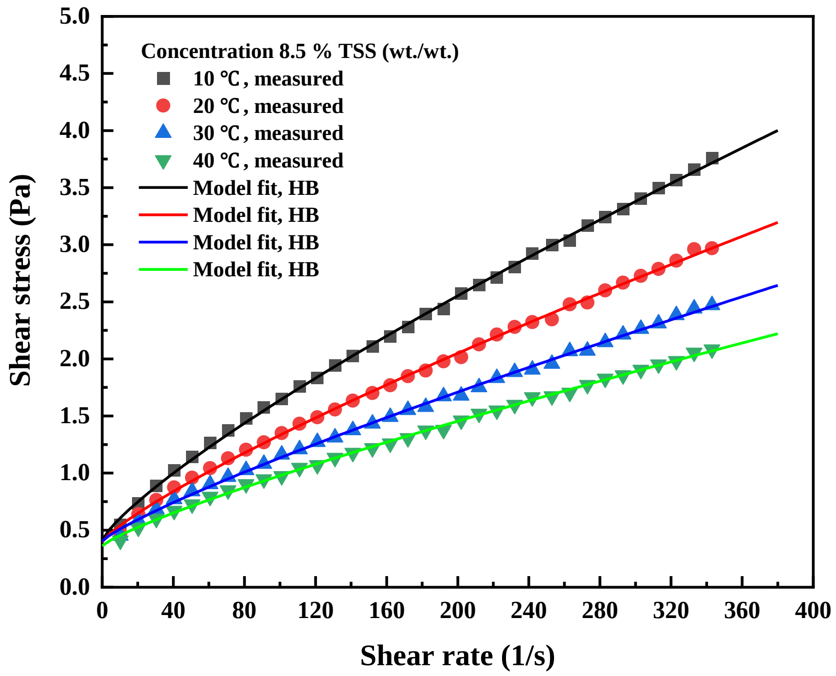
Concentration 8.5 % TSS (wt./wt.)
10 ℃, measured
20 ℃, measured
30 ℃, measured
40 ℃, measured
Model fit, HB
Model fit, HB
Model fit, HB
Model fit, HB
Shear stress (Pa)
Shear rate (1/s)
0.0
0.5
1.0
1.5
2.0
2.5
3.0
3.5
4.0
4.5
5.0
0 40 80 120 160 200 240 280 320 360 400

(e)

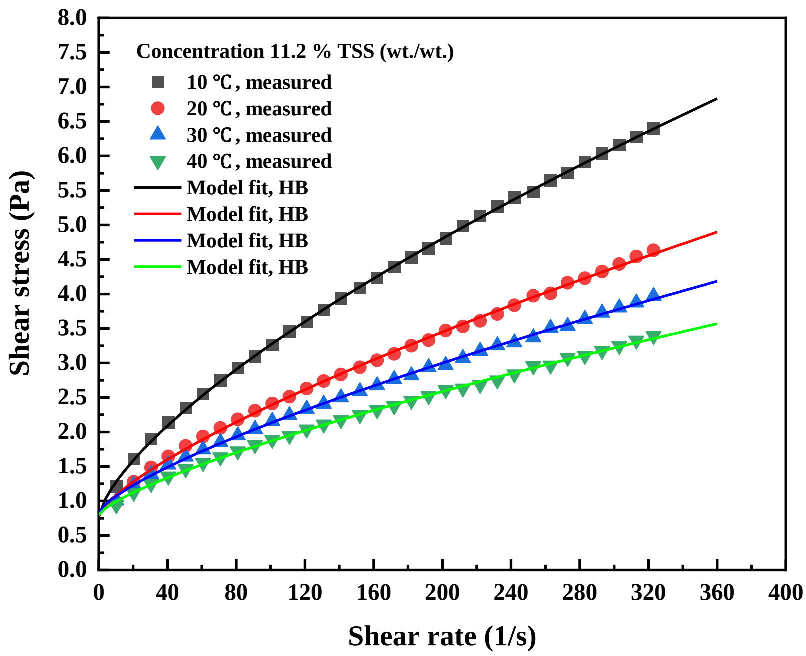

(f)

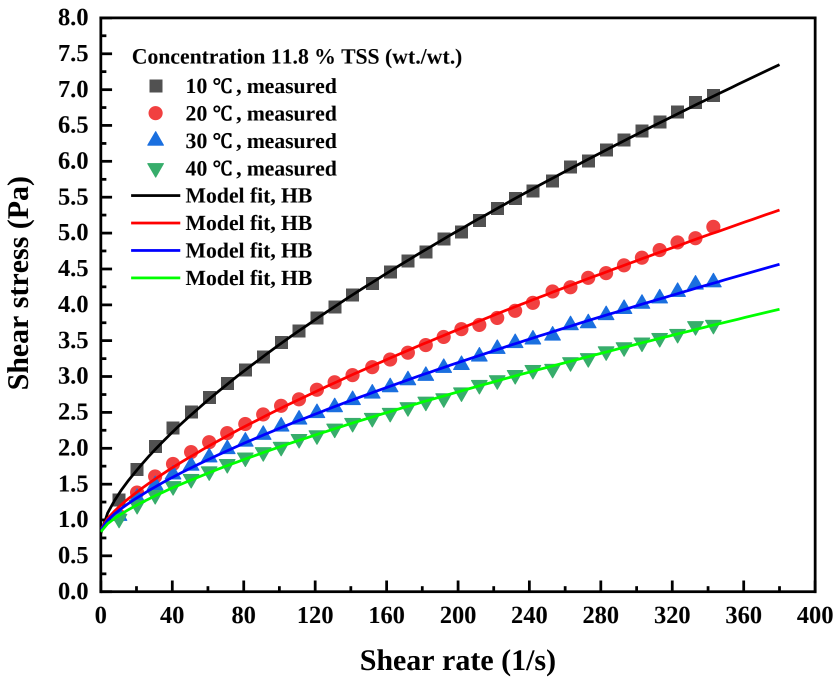

(g)

Figure 4. The rheograms for urine sludge at various concentrations and temperatures

3.2. Effect of temperature

Temperature changes influenced the rheological behavior of sludge (Baudez et al., 2013; Thota Radhakrishnan et al., 2018). In general, an increase in temperature resulted in a decrease in sludge viscosity (Eshtiaghi et al., 2013). Similar phenomenon was observed in this work. Based on the rheograms (Figure 4), for each sample at a given shear rate, the shear stress decreased with increasing temperature, indicating a lower apparent viscosity at higher temperatures. This can be explained by that at low shear rates the apparent viscosity was dominated by the interparticle interaction. The increasing temperature resulted in the decrease in the interactive forces between particles lowing the apparent viscosity (Mikulášek et al., 1997). Thota Radhakrishnan et al. (2018) also showed that the increasing temperature led to the increase in thermal motion of the molecules, which reduced the forces between the molecules, thereby resulting in a low apparent viscosity.

In this work, modeling of the temperature effect was conducted using Origin 2021 software to provide a comprehensive understanding of the influence of temperature on the rheological behavior of urine sludge. The temperature effect on sludge viscosity could be described well with an Arrhenius-type equation (5) (Abu-Jdayil et al., 2010; de Kretser and Scales, 2008; Eshtiaghi et al., 2013; Pevere et al., 2009; Thota Radhakrishnan et al., 2018):

$$\eta_\infty = Ke^{\frac{E_a}{RT}} \tag{5}$$

where η_∞ is the limiting viscosity; K is the empirical constant; T is the absolute temperature; R is the universal gas constant, and E_a is the activation energy. The limiting viscosity data were obtained using the rheological measurement approach mentioned in section 2.2. The relationship between urine sludge viscosity and temperature at various concentrations was presented in Figure 5. Table 4 shows the regressed parameters of equation 5 at various concentrations. The results showed that the Arrhenius-type equation was able to describe the influence of the temperature on the rheology of urine sludge at various concentrations.

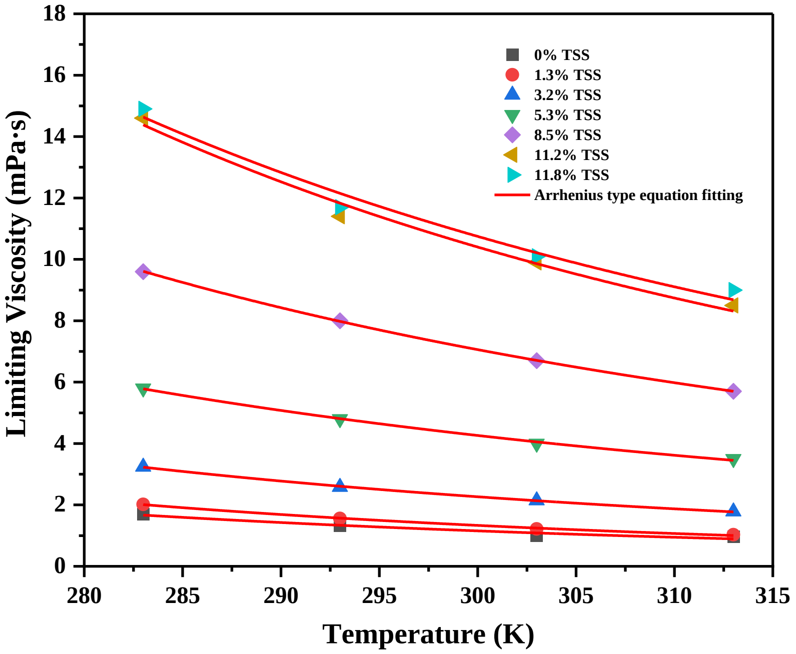

Figure 5. The relationship between urine sludge viscosity and temperature at various concentrations

Table 4. Regressed parameters of equation 5.

% TSS	K (mPa·s)	$\frac{E_a}{R}$ (K)	R^2
0	0.00249	1842.2316	0.96005
1.3	0.00142	2053.04331	0.99725

3.2	0.00619	1770.6861	0.99913
5.3	0.02655	1523.57141	0.99815
8.5	0.04157	1540.38635	0.99993
11.2	0.04732	1617.83707	0.98683
11.8	0.06306	1541.50924	0.98036

3.3. Effect of TSS concentration

The effect of solid content on the rheological behavior of sludge has been discussed in many studies (Eshtiaghi et al., 2013; Thiène et al., 2019; Thota Radhakrishnan et al., 2018; Wang et al., 2016). Dilute sludge behaved similar to a Newtonian fluid; however, the rheological behavior became non-Newtonian when the solid concentration increased (Eshtiaghi et al., 2013; Thiène et al., 2019). Similar results were obtained in this work. Based on the rheograms in Figure 4, the shear stress increased linearly with the shear rate at TSS concentrations ≤ 3.2% in urine sludge. The Newtonian/Bingham models were able to describe the rheological behavior of diluted urine sludge. At TSS concentrations ≥ 5.3%, urine sludge exhibited non-Newtonian behavior, and the HB model could be used to describe the high-concentration sludge. In this study, the effect of concentration on the rheological behavior of urine sludge was investigated through correlating the rheological parameters with the solid concentrations of sludge.

3.3.1. Effect of TSS concentration on the limiting viscosity

An empirical exponential model (Figure 6) was used to describe the relationship between the limiting viscosity of urine sludge and TSS concentrations at 10 °C, 20 °C, 30 °C, and 40 °C. This model has already been reported in other work (Mu and Yu, 2006). The regression coefficient, which varied from 0.98145 to 0.98822, indicated that this exponential model was able to adequately describe such a relationship. The limiting viscosity increased with increasing urine sludge concentration. Many studies have investigated the effect of solid content on the limiting viscosity of sludge. In general, the limiting viscosity of sludge increased with increasing solid content (Abu-Jdayil et al., 2010; Moreau et al., 2009; Mu and Yu, 2006). The presence and concentration of solids have been considered as the primary reasons for the increased viscosity, which can be explained by the following Einstein's Law of Viscosity (equation 6):

$$\eta/\eta_0 = 1 + 2.5\,\phi \tag{6}$$

where η is the viscosity; η_0 is the viscosity of the fluid phase, and ϕ is the particle volume fraction. Einstein's theory indicated that the solids suspended in the fluid were spherical, non-interacting, insoluble, and rigid (Sanin, 2002). For the same particle-size distribution condition of urine sludge, the number of particles increased with increasing TSS concentration, leading to strong inter-particle interactions and increased viscosity (Pevere et al., 2006).

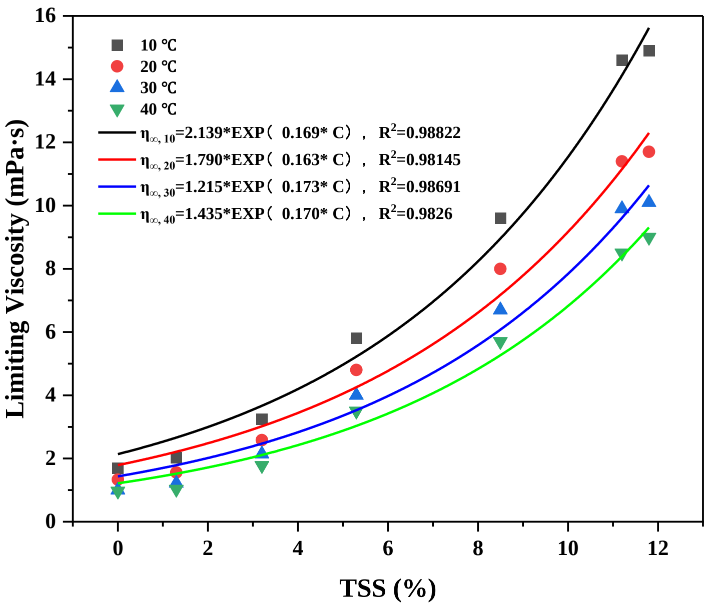

Figure 6. The relationship between urine sludge viscosity and concentration at temperature 10 ℃, 20 ℃, 30 ℃, and 40 ℃.

3.3.2. Effect of TSS concentration on yield stress (τ_0)

Yield stress is an important parameter to characterize the rheological behavior of sludge. It is defined as the minimum applied stress required for the sludge to start flowing. In this work, the yield stress values were calculated by the extrapolation of flow curve to zero shear rate using the rheological models of sludge (Eshtiaghi et al., 2013). The effect of solid concentration on the yield stress of sludge has been discussed in many studies. In general, yield stress was 0, which is below a threshold concentration, and then it increased with the increase of solid concentrations (Baudez et al., 2011; Eshtiaghi et al., 2013; Mori et al., 2006; Thota Radhakrishnan et al., 2018). Yield stress was a static quantity, which was governed by the interparticle forces and network structure (de Kretser and Scales, 2008). Increasing the concentration led to the increase in particle interactions, which increased the number of neighboring particle interactions, thereby creating a structure (Thota

Radhakrishnan et al., 2018). Increasing the concentration modified the relative intensity of interactions between solid particles (Baudez et al., 2011). At TSS concentrations ≤ 1.3%, the yield stress of urine sludge was 0. At TSS concentrations ≥ 3.2%, a power law (Baudez et al., 2011) was used to describe the effect of concentration on the yield stress of urine sludge (Figure 7).

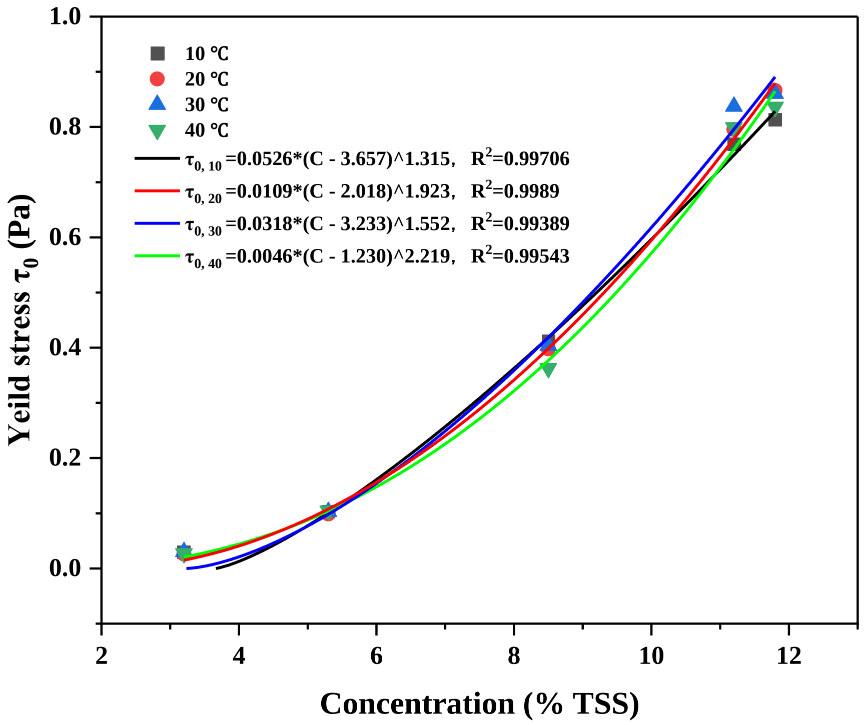

Figure 7. A power-law representing the effect of concentration on yield stress at temperature 10 ℃, 20 ℃, 30 ℃, and 40 ℃.

3.3.3. Effect of TSS concentration on consistency index (K)

The consistency index (K) has been proven to be an important indicator of the rheological behavior, which could be used to describe the viscous behavior of the sludge (Eshtiaghi et al., 2013; Thota Radhakrishnan et al., 2018). Many studies have shown the correlation between “K” and concentration of sludge (Moreau et al., 2009; Mori et al., 2006; Thota Radhakrishnan et al., 2018).

In this work, an exponential law was used to represent the effect of concentration on the consistency index (K) at 10 °C, 20 °C, 30 °C, and 40 °C (Figure 8). The consistency index (K) increased with the increase of urine sludge concentration. The regression coefficient, which varied from 0.99334 to 0.99966, indicated that this exponential model could represent such a correlation. The exponential behavior of “K” in sludge could be explained by the increase in particle interactions with the increase of concentration (Thota Radhakrishnan et al., 2018).

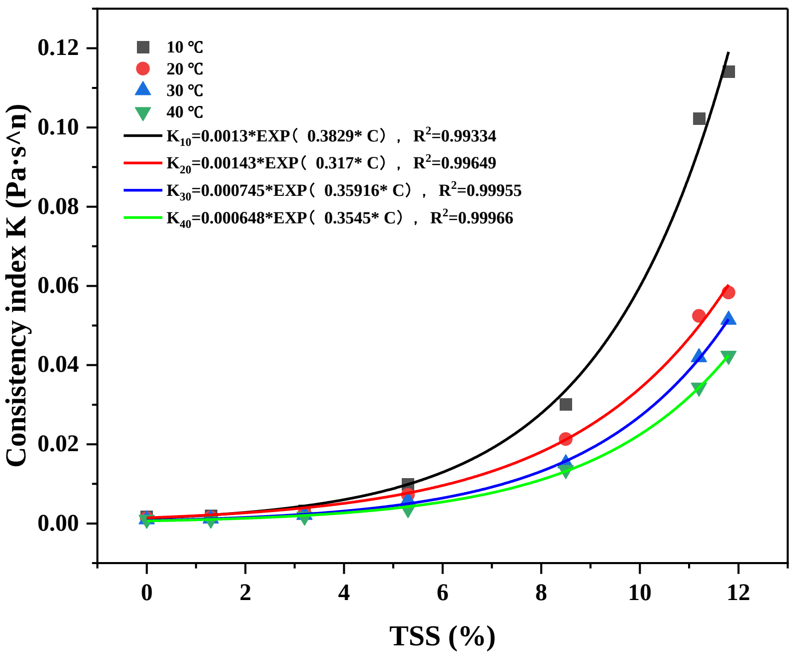

Figure 8. An exponential law representing the effect of concentration on consistency index K at temperature 10 ℃, 20 ℃, 30 ℃, and 40 ℃.

3.3.4. Effect of TSS concentration on behavior index (n)

The behavior index is an important parameter because it describes the relationship between the shear rate and shear stress. In this work, the effect of concentration on the behavior index was investigated.

At TSS concentrations ≤ 3.2%, urine sludge had the behavior index of 1, which indicated a linear increase function in shear stress with regard to the shear rate. At TSS concentrations ≥ 5.3%, urine sludge with the behavior index of less than 1 presented shear thinning behavior, which occurred with the breakup of the fluid structures and constituent particles aligning in the direction of the flow (Thota Radhakrishnan et al., 2018). The shearing forces tended to break the fluid structures. As the shearing rate increased, more fluid structures were broken, and the suspended particles aligned with the sludge flow, thereby presenting shear thinning behavior. Moreover, the behavior index reflected the intensity of sludge in the non-linear regime (Wang et al., 2016). Taking the rheological data obtained at 20 °C as an example, the behavior index (n) decreased from 0.91227 to 0.72987 as the TSS concentrations increased from 5.3% to 11.8%, indicating that the non-Newtonian flow characteristics of urine sludge were strengthened at high TSS concentration. Thus, the increase in concentration led to an increase in the fluid structures presented in sludge and resulted in a high proportion of broken fluid structures at high shearing rate, which presented increased shear thinning behavior (Thota Radhakrishnan et al., 2018).

Many researchers have attempted to correlate the behavior index (n) with the TSS concentration of sludge. A polynomial (Slatter, 1997), linear (Mori et al., 2006), or power-law function (Moreau et al., 2009) has been reported to describe such a correlation. At TSS concentrations ≤ 3.2%, the behavior index (n) of urine sludge was 1. At TSS concentrations ≥ 5.3%, a linear model was used to represent the effect of concentration on the behavior index (n) at 10 °C, 20 °C, 30 °C, and 40 °C (Figure 9). The regression coefficient, which varied from 0.98712 to 0.99909, indicated that the linear model could represent such a correlation.

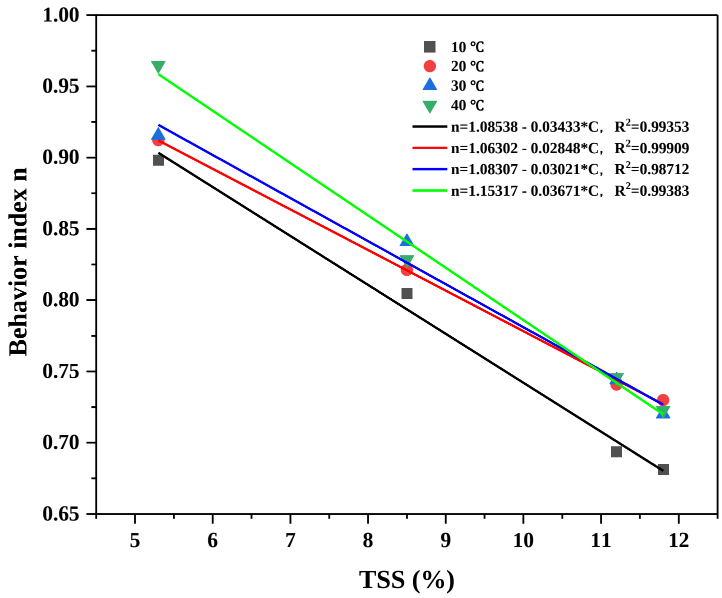

Figure 9. A linear model representing the effect of concentration on consistency index K at temperature 10 ℃, 20 ℃, 30 ℃, and 40 ℃.

3.4. Discussion

Microbial ureolysis occurred in urine diversion systems leads to the increase of the pH, which results in the formation of phosphorus-based solids. The gravitational sedimentation leads to a large solid concentration gradient in the horizontal pipelines. The variability in the urine sludge rheological characteristics as a result of the variability in solid concentration will increase the difficulty for engineers to design and optimize piping systems. In urine diversion systems, a small increase in urine sludge concentration might increase the transition velocity from turbulent to laminar flow (Eshtiaghi et al., 2012). Ignoring the rheological characteristics of fluids would make engineers to misjudge the pressure drop and flow regime (laminar or turbulent). This misjudgment may cause the fluid behavior in the pipeline to change from turbulent flow to laminar flow, which is undesirable because it increases the risk of suspended solids deposition. On the other hand, the fluidity of the sludge becomes worser as the viscosity increases (Ratkovich et al., 2013). In urine diversion systems, for a given pipe slope or pumping power, the increased viscosity results in the decrease of the fluid velocity. A lower fluid velocity will increase the residence time of urine sludge in the pipeline, allowing sufficient time for suspended solids to settle to the bottom of the pipe. A lower fluid velocity also leads to the decrease of the wall shear stress. The deposited solids cannot get enough shear force to move forward with the flow, which leads to the continuous increase of the sludge solid concentration in the sedimentation layer, and eventually causing pipe blockage.

The non-Newtonian rheological characteristics of urine sludge will strongly influence the flow behavior. This study found that above the threshold concentration, urine sludge showed the presence of yield stress, and it increased with the increase of solid concentration. Shear stress distribution in circular laminar pipe flow can be described as follows (Farno et al., 2018):

$$\tau = \left(-\frac{\Delta P}{L}\right)\frac{r}{2} \quad (7)$$

where ΔP (Pa) is the pressure difference.

It shows that the shear stress is distributed linearly along the radius. Therefore, there might be an area close to the pipe center where the yield stress of the sludge is more than the actual shear stress it experiences. In this area where the shear force is small, the sludge might remain unsheared in the presence of the yield stress, and this part of the sludge moves as a solid plug in the presence of yield stress, which might have an impact on the stability of flow (Eshtiaghi et al., 2012). Baudez (2008) proposed that the sludge starts to flow as soon as the critical shear stress is reached but the flow is homogeneous only when another higher critical shear stress is reached. Otherwise, the solids structure tends to rebuild due to colloidal forces even under shear. In pipe transportation, thixotropic effects of the sludge will lead to blockage if the wall shear stress is not high enough to maintain a homogenous flow, and this situation would become more serious with the increasing solid concentration because the critical shear stress for homogenous flow is a power law function of solids concentration (Eshtiaghi et al., 2013).

In this work, the relationship between urine sludge viscosity and temperature at various concentrations was described using an Arrhenius-type equation. It was found that a decrease in temperature will result in an increase in viscosity of urine sludge, especially at high solids concentrations. Baudez et al. (2013) suggested that the temperature dependent properties of sludge should be taken into account in the hydrodynamic modelling in industrial flow processes in which temperature changes, to accurately determine the head loss. In urine diversion systems, the impacts of temperature on urine sludge viscosity may be a result of the temperature difference between indoor and outdoor pipelines caused by the change of seasons.

Based on the comparison with available literature data (Baudez et al., 2011; Markis et al., 2014; Thota Radhakrishnan et al., 2018), it was found that urine sludge presented similar non-Newtonian characteristics to primary sludge, secondary sludge, anaerobic digested sludge and concentrated black water. Therefore, this study suggested that last experiences on the design and optimization of pipe transportation for municipal sewage treatment plants could provide valuable information for urine diversion implementation on city-scale, especially on how to accurately calculate the pressure drop and avoid pipe blockage.

4. Conclusion

As a result of the gravitational sedimentation, the large solid concentration gradient leads to the variability in the rheological characteristics of urine sludge. The urine sludge behaved like a Newtonian fluid at lower TSS concentrations. With the increase of the TSS concentrations, urine sludge was a shear thinning fluid and showed the presence of yield stress, which could be modeled using the Herschel–Bulkley model. Ignoring the rheological characteristics of urine sludge would make engineers to misjudge the pressure drop and flow regime (laminar or turbulent), which increases the risk of pipe blockage. The apparent viscosity of urine sludge decreased with increasing temperature. An Arrhenius-type equation was used to describe the effect of temperature on sludge viscosity. In urine diversion systems, engineers should consider the temperature difference between indoor and outdoor pipes as a result of the seasonal changes, which would affect the rheological characteristic of the urine sludge. Since urine sludge presented similar non-Newtonian characteristics to municipal wastewater sludge, previous experiences on the design and optimization of pipe transportation for municipal sewage treatment plants could provide valuable information for urine diversion implementation on city-scale, especially on how to accurately calculate the pressure drop and avoid pipe blockage.

Acknowledgement

This work was supported by National Key Research and Development Plan (2017YFC0403401), Natural Science Foundation of China (51808036) and the Bill and Melinda Gates Foundation (Research Development and technical assistance to RTTC-China Project (OPP1161151) & Reinvent the Toilet China Project: Innovative Toilet Solutions and Commercial Activities (OPP1157726)). The authors would like to take this opportunity to express our sincere appreciation for the support of National Environment and Energy International Science and Technology Cooperation Base.

References:

Abu-Jdayil, B., Banat, F., Al-Sameraiy, M., 2010. Steady Rheological Properties of Rotating Biological Contactor (RBC) Sludge. Journal of Water Resource and Protection 02(01), 1-7.

Baudez, J.C., 2008. Physical Aging and Thixotropy in Sludge Rheology. Appl. Rheol. 18(1), 13491-13495.

Baudez, J.C., Markis, F., Eshtiaghi, N., Slatter, P., 2011. The rheological behaviour of anaerobic digested sludge. Water Res. 45(17), 5675-5680.

Baudez, J.C., Slatter, P., Eshtiaghi, N., 2013. The impact of temperature on the rheological behaviour of anaerobic digested sludge. Chem. Eng. J. 215-216, 182-187.

Boyer, T.H., Saetta, D., 2019. Opportunities for Building-Scale Urine Diversion and Challenges for Implementation. Accounts Chem. Res. 52(4), 886-895.

Chipako, T.L., Randall, D.G., 2020. Investigating the feasibility and logistics of a decentralized urine treatment and resource recovery system. Journal of Water Process Engineering 37, 101383.

Christiaens, M.E.R., De Vrieze, J., Clinckemaillie, L., Ganigué, R., Rabaey, K., 2019. Anaerobic ureolysis of source-separated urine for NH3 recovery enables direct removal of divalent ions at the toilet. Water Res. 148, 97-105.

de Kretser, R.G., Scales, P.J., 2008. The effect of temperature on the yield stress of mineral suspensions. J. Colloid Interf. Sci. 328(1), 187-193.

Dodane, P., Mbéguéré, M., Sow, O., Strande, L., 2012. Capital and Operating Costs of Full-Scale Fecal Sludge Management and Wastewater Treatment Systems in Dakar, Senegal. Environ. Sci. Technol. 46(7), 3705-3711.

Eshtiaghi, N., Markis, F., Slatter, P., 2012. The laminar/turbulent transition in a sludge pipeline. Water Sci. Technol. 65(4), 697-702.

Eshtiaghi, N., Markis, F., Yap, S.D., Baudez, J., Slatter, P., 2013. Rheological characterisation of municipal sludge: A review. Water Res. 47(15), 5493-5510.

Farno, E., Coventry, K., Slatter, P., Eshtiaghi, N., 2018. Role of regression analysis and variation of rheological data in calculation of pressure drop for sludge pipelines. Water Res. 137, 1-8.

Hellström, D., Johansson, E., Grennberg, K., 1999. Storage of human urine: acidification as a method to inhibit decomposition of urea. Ecol. Eng. 12(3), 253-269.

Kavvada, O., Tarpeh, W.A., Horvath, A., Nelson, K.L., 2017. Life-Cycle Cost and Environmental Assessment of Decentralized Nitrogen Recovery Using Ion Exchange from Source-Separated Urine through Spatial Modeling. Environ. Sci. Technol. 51(21), 12061-12071.

Markis, F., Baudez, J., Parthasarathy, R., Slatter, P., Eshtiaghi, N., 2014. Rheological characterisation of primary and secondary sludge: Impact of solids concentration. Chem. Eng. J. 253, 526-537.

Mikulášek, P., Wakeman, R.J., Marchant, J.Q., 1997. The influence of pH and temperature on the rheology and stability of aqueous titanium dioxide dispersions. Chem. Eng. J. 67(2), 97-102.

Moreau, A.A., Ratkovich, N., Nopens, I., van der Graaf, J.H.J.M., 2009. The (in)significance of apparent viscosity in full-scale municipal membrane bioreactors. J. Membrane Sci. 340(1-2), 249-256.

Mori, M., Seyssiecq, I., Roche, N., 2006. Rheological measurements of sewage sludge for various solids concentrations and geometry. Process Biochem. 41(7), 1656-1662.

Mu, Y., Yu, H., 2006. Rheological and fractal characteristics of granular sludge in an upflow anaerobic reactor. Water Res. 40(19), 3596-3602.

Pevere, A., Guibaud, G., Goin, E., van Hullebusch, E., Lens, P., 2009. Effects of physico-chemical factors on the viscosity evolution of anaerobic granular sludge. Biochem. Eng. J. 43(3), 231-238.

Pevere, A., Guibaud, G., van Hullebusch, E., Lens, P., Baudu, M., 2006. Viscosity evolution of anaerobic granular sludge. Biochem. Eng. J. 27(3), 315-322.

Randall, D.G., Krähenbühl, M., Köpping, I., Larsen, T.A., Udert, K.M., 2016. A novel approach for stabilizing fresh urine by calcium hydroxide addition. Water Res. 95, 361-369.

Ratkovich, N., Horn, W., Helmus, F.P., Rosenberger, S., Naessens, W., Nopens, I., Bentzen, T.R., 2013. Activated sludge rheology: A critical review on data collection and modelling. Water Res. 47(2), 463-482.

Rooki, R., Ardejani, F.D., Moradzadeh, A., Mirzaei, H., Kelessidis, V., Maglione, R., Norouzi, M., 2012. Optimal determination of rheological parameters for herschel-bulkley drilling fluids using genetic algorithms (GAs). Korea-Aust. Rheol. J. 24(3), 163-170.

Saetta, D., Padda, A., Li, X., Leyva, C., Mirchandani, P.B., Boscovic, D., Boyer, T.H., 2019. Real-Time Monitoring and Control of Urea Hydrolysis in Cyber-Enabled Nonwater Urinal System. Environ. Sci. Technol. 53(6), 3187-3197.

Sanin, F.D., 2002. Effect of solution physical chemistry on the rheological properties of activated sludge. Water SA 28(2), 207-212.

Seyssiecq, I., Ferrasse, J., Roche, N., 2003. State-of-the-art: rheological characterisation of wastewater treatment sludge. Biochem. Eng. J. 16(1), 41-56.

Slatter, P.T., 1997. The rheological characterisation of sludges. Water Sci. Technol. 36(11), 9-18.

Thiène, O., Dieudé-Fauvel, E., Baudez, J.C., 2019. Impact of mechanical history on sludge rheological properties: Role of the organic content. Water Res. 157, 175-180.

Thota Radhakrishnan, A.K., Alidai, A., Pothof, I., Lier, J.V., Clemens, F., 2015. Predicting the onset of secondary flows in the rheological measurement of domestic slurry.

Thota Radhakrishnan, A.K., van Lier, J.B., Clemens, F.H.L.R., 2018. Rheological characterisation of concentrated domestic slurry. Water Res. 141, 235-250.

Tove, A., Larsen, Sabine, Hoffmann, Christoph, Lüthi, Bernhard, Truffer, Max, Maurer, 2016. Emerging solutions to the water challenges of an urbanizing world. Science (New York, N.Y.).

Udert, K.M., Larsen, T.A., Biebow, M., Gujer, W., 2003. Urea hydrolysis and precipitation dynamics in a urine-collecting system. Water Res. 37(11), 2571-2582.

Udert, K.M., Larsen, T.A., Gujer, W., 2003a. Estimating the precipitation potential in urine-collecting systems. Water Res. 37(11), 2667-2677.

Udert, K.M., Larsen, T.A., Gujer, W., 2003b. Biologically induced precipitation in urine-collecting systems. Water Sci. Technol. 3(3), 71-78.

Wang, H., Hu, H., Yang, H., Zeng, R.J., 2016. Characterization of anaerobic granular sludge using a rheological approach. Water Res. 106, 116-125.

Graphical Abstract

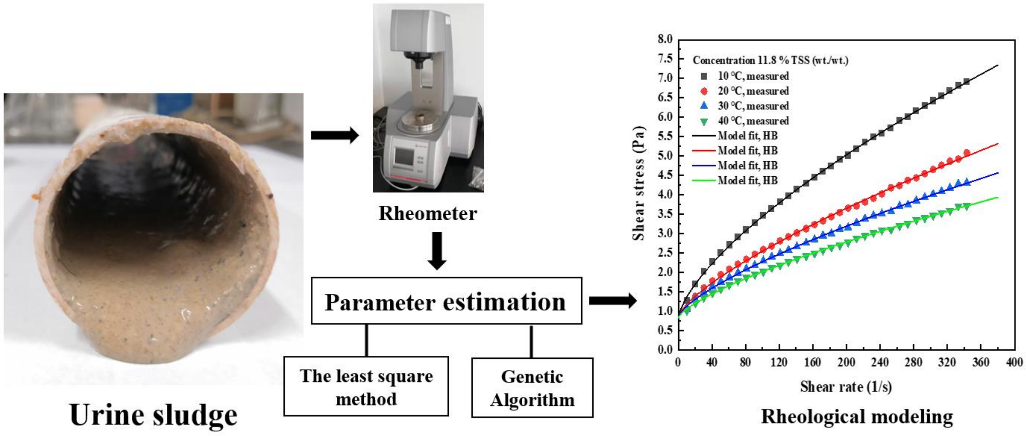

Declaration of interests

✓ The authors declare that they have no known competing financial interests or personal relationships that could have appeared to influence the work reported in this paper.

☐The authors declare the following financial interests/personal relationships which may be considered as potential competing interests:

TO: Editor of **Resources Conservation &Recycling**

Dear Editor,

This is to submit a Research Paper entitled "**The effect of temperature and concentration of urine sludge on rheological characterization**" for the consideration of publication in **Resources Conservation &Recycling**. This paper aimed to understand the basic characteristics of the rheological behavior of urine sludge and provide important parameters to improve the design of the urine transported pipe systems. In this work, the rheograms obtained from experimental rheological measurements had been used to build viscosity models. The effect of concentration and temperature on the rheological behavior of urine sludge was investigated through correlating the rheological parameters with concentrations and temperatures. The effect of the variability in the urine sludge rheological characteristics on the design and optimization of piping systems is discussed.

We confirm that this manuscript has not been published elsewhere and is not under consideration by any other journal. All authors have approved the manuscript and agree with this submission.

A professional English-language services company has copy edited this paper to improve its readability.

Please feel free to contact if there is any question regarding the article. Thanks a lot for your assistance in processing our submission. It is highly appreciated.

Best regards,

Zifu Li

Address:University of Science and Technology Beijing, Xueyuan Road No.30, Haidian District, Beijing-100083, P.R. China.

E-mail: zifulee@aliyun.com.

Tel: +86-010-62334378

Fax: +86-010-62334378

Supplementary Tables

Table A1. The rheometric data fits obtained from Origin 2021 software

Concentration	Temperature	Model	Adjusted R Square	τ_0	K	n
% TSS (wt./wt.)	℃	-	-	Pa	Pa·s^n	-
0	10	Newtonian	0.99736	0	0.00169	1
		Ostwald	0.99366	0	0.00105	1.09839
		Bingham	0.98515	0	0.00174	1
		HB	0.99345	0.00554	0.000810641	1.14576
	20	Newtonian	0.99504	0	0.00133	1
		Ostwald	0.98515	0	0.000799112	1.10977
		Bingham	0.97476	0	0.00138	1
		HB	0.98431	0.00522	0.000550884	1.18096
	30	Newtonian	0.99472	0	0.001	1
		Ostwald	0.97513	0	0.000981904	1.00451
		Bingham	0.97501	0	0.00101	1
		HB	0.97099	0	0.000975321	1.0061
	40	Newtonian	0.99417	0	0.000970983	1
		Ostwald	0.97762	0	0.000712185	1.07154
		Bingham	0.9708	0	0.000999891	1
		HB	0.97442	0	0.000710086	1.07231
1.3	10	Newtonian	0.99874	0	0.00202	1

		Ostwald	0.99487	0	0.00234	0.9695
		Bingham	0.99454	0.0027	0.002	1
		HB	0.9945	0	0.00236	0.96809
	20	Newtonian	0.9976	0	0.00156	1
		Ostwald	0.99334	0	0.00104	1.08466
		Bingham	0.98751	0	0.0016	1
		HB	0.99349	0.00804	0.00067479	1.16545
	30	Newtonian	0.99478	0	0.00122	1
		Ostwald	0.97632	0	0.00144	0.9614
		Bingham	0.97544	0.000455499	0.00121	1
		HB	0.97257	0	0.00159	0.93935
	40	Newtonian	0.99575	0	0.00103	1
		Ostwald	0.98279	0	0.000813297	1.05311
		Bingham	0.98129	0	0.00103	1
		HB	0.98087	0.00236	0.000636635	1.10161
3.2	10	Newtonian	0.99815	0	0.00348	1
		Ostwald	0.99686	0	0.00568	0.89987
		Bingham	0.99804	0.02957	0.00324	1
		HB	0.99791	0.02973	0.00323	1.0007
	20	Newtonian	0.99784	0	0.00279	1
		Ostwald	0.99544	0	0.00461	0.89753
		Bingham	0.99807	0.02614	0.00258	1
		HB	0.99829	0.03627	0.00186	1.06052
	30	Newtonian	0.99627	0	0.00239	1
		Ostwald	0.99496	0	0.00496	0.85036

		Bingham	0.99715	0.03003	0.00214	1
		HB	0.99698	0.02841	0.00228	0.98913
	40	Newtonian	0.99538	0	0.002	1
		Ostwald	0.99139	0	0.0043	0.84308
		Bingham	0.99488	0.02699	0.00178	1
		HB	0.99459	0.02971	0.00157	1.02264
5.3	10	Newtonian	0.99389	0	0.00621	1
		Ostwald	0.99696	0	0.01909	0.79141
		Bingham	0.99743	0.16935	0.00539	1
		HB	0.99841	0.1027	0.00987	0.89847
	20	Newtonian	0.99323	0	0.00498	1
		Ostwald	0.996	0	0.01609	0.78231
		Bingham	0.99742	0.14381	0.00428	1
		HB	0.99814	0.09836	0.00725	0.91164
	30	Newtonian	0.99105	0	0.00415	1
		Ostwald	0.99375	0	0.01568	0.75287
		Bingham	0.9965	0.13788	0.00348	1
		HB	0.99711	0.10281	0.00575	0.91562
	40	Newtonian	0.90123	0	0.00355	1
		Ostwald	0.991	0	0.01282	0.76124
		Bingham	0.99636	0.11641	0.00298	1
		HB	0.99633	0.1055	0.00361	0.96761
8.5	10	Newtonian	0.9804	0	0.01205	1
		Ostwald	0.99497	0	0.09025	0.63363
		Bingham	0.99517	0.68395	0.0091	1

		HB	0.99925	0.4118	0.03013	0.80466
	20	Newtonian	0.97763	0	0.00966	1
		Ostwald	0.99236	0	0.08155	0.61184
		Bingham	0.99534	0.5889	0.00713	1
		HB	0.99868	0.39785	0.02129	0.82121
	30	Newtonian	0.97349	0	0.00805	1
		Ostwald	0.98884	0	0.08018	0.58147
		Bingham	0.99589	0.53733	0.00574	1
		HB	0.99846	0.40388	0.01516	0.84101
	40	Newtonian	0.97027	0	0.00683	1
		Ostwald	0.98802	0	0.07666	0.55945
		Bingham	0.99543	0.48348	0.00474	1
		HB	0.99851	0.36191	0.01361	0.82768
11.2	10	Newtonian	0.96763	0	0.02281	1
		Ostwald	0.99608	0	0.27243	0.54331
		Bingham	0.98884	1.57536	0.01561	1
		HB	0.99972	0.76938	0.10226	0.69355
	20	Newtonian	0.96235	0	0.01641	1
		Ostwald	0.9907	0	0.23237	0.51165
		Bingham	0.99139	1.23471	0.01077	1
		HB	0.99865	0.79485	0.05248	0.74052
	30	Newtonian	0.95423	0	0.01423	1
		Ostwald	0.98732	0	0.25358	0.46901
		Bingham	0.99183	1.19005	0.00879	1
		HB	0.99905	0.83573	0.04215	0.74324

	40	Newtonian	0.9488	0	0.01226	1
		Ostwald	0.98447	0	0.25089	0.44322
		Bingham	0.99175	1.08857	0.00728	1
		HB	0.99879	0.79893	0.03437	0.74571
11.8	10	Newtonian	0.96672	0	0.02328	1
		Ostwald	0.99628	0	0.29516	0.53735
		Bingham	0.98785	1.72828	0.01584	1
		HB	0.99969	0.813328	0.11409	0.68145
	20	Newtonian	0.96129	0	0.01692	1
		Ostwald	0.99069	0	0.25534	0.50531
		Bingham	0.99061	1.36912	0.01102	1
		HB	0.99851	0.86759	0.0581	0.73048
	30	Newtonian	0.95457	0	0.01472	1
		Ostwald	0.98911	0	0.26869	0.47041
		Bingham	0.99034	1.29846	0.00913	1
		HB	0.99912	0.86061	0.05139	0.72016
	40	Newtonian	0.94936	0	0.01281	1
		Ostwald	0.98679	0	0.26758	0.44563
		Bingham	0.99063	1.19847	0.00765	1
		HB	0.99934	0.83618	0.04236	0.72276

Table A2. The rheometric data fits obtained from genetic algorithm

Concentration	Temperature	Model	RMSE	τ_0	K	n
% TSS (wt./wt.)	℃	-	-	Pa	Pa·s^n	-

0	10	Newtonian	0.00873409	0	0.00169065	1
		Ostwald	0.00677366	0	0.0010497	1.09833403
		Bingham	0.00873409	0	0.00169065	1
		HB	0.00665008	0.00551929	0.00081152	1.14556445
	20	Newtonian	0.00778394	0	0.00133227	1
		Ostwald	0.00669796	0	0.00079948	1.10966942
		Bingham	0.00778394	0	0.00133226	1
		HB	0.00659289	0.00520189	0.00055167	1.18042753
	30	Newtonian	0.00391316	0	0.00100008	1
		Ostwald	0.00391223	0	0.00098172	1.00454996
		Bingham	0.00391316	0	0.0010008	1
		HB	0.00391223	0	0.00098313	1.0042129
	40	Newtonian	0.00442537	0	0.00097096	1
		Ostwald	0.00418753	0	0.00071192	1.07161705
		Bingham	0.00442537	0	0.00097097	1
		HB	0.00418753	0	0.00071198	1.07159469
1.3	10	Newtonian	0.00721567	0	0.00202282	1
		Ostwald	0.00688350	0	0.00234416	0.96953595
		Bingham	0.00709923	0.00270142	0.0019999	1
		HB	0.00688351	0	0.00234303	0.96963528
	20	Newtonian	0.00724730	0	0.00156318	1
		Ostwald	0.00596354	0	0.00104281	1.08456623
		Bingham	0.00709923	0.00270142	0.0019999	1
		HB	0.00568118	0.00845663	0.00065535	1.17101065
	30	Newtonian	0.00525896	0	0.00121946	1

		Ostwald	0.00515924	0	0.0014403	0.96153601
		Bingham	0.00525473	0.00045667	0.001213	1
		HB	0.00515926	0	0.00143694	0.96207302
	40	Newtonian	0.00438864	0	0.00102865	1
		Ostwald	0.00422000	0	0.00081355	1.05304108
		Bingham	0.00438864	0	0.00102865	1
		HB	0.00419501	0.00233337	0.00063907	1.10084075
3.2	10	Newtonian	0.01594061	0	0.00347951	1
		Ostwald	0.00925364	0	0.00568001	0.8998091
		Bingham	0.00730515	0.02956931	0.00324227	1
		HB	0.00730506	0.02973184	0.00322942	1.00072858
	20	Newtonian	0.01379750	0	0.00279113	1
		Ostwald	0.00887106	0	0.00460975	0.89741864
		Bingham	0.00577995	0.02614734	0.00258134	1
		HB	0.00526499	0.03629434	0.00185707	1.06065987
	30	Newtonian	0.01552348	0	0.00238522	1
		Ostwald	0.00775036	0	0.00495905	0.85026616
		Bingham	0.00582594	0.0300288	0.00214429	1
		HB	0.00581483	0.02842623	0.00227355	0.9892661
	40	Newtonian	0.01447385	0	0.00199775	1
		Ostwald	0.00842269	0	0.00430394	0.84296751
		Bingham	0.00649606	0.02699365	0.00178117	1
		HB	0.00646768	0.02998556	0.00155471	1.02498652
5.3	10	Newtonian	0.08582643	0	0.00620977	1
		Ostwald	0.02553582	0	0.01909822	0.79134721

		Bingham	0.02348756	0.16935128	0.00538537	1
		HB	0.01814189	0.10269181	0.00987139	0.89845639
	20	Newtonian	0.07255708	0	0.00498325	1
		Ostwald	0.02330644	0	0.01609544	0.78222403
		Bingham	0.01871840	0.14381151	0.00428318	1
		HB	0.01560052	0.09871291	0.00722623	0.91227097
	30	Newtonian	0.06949739	0	0.00414714	1
		Ostwald	0.02365118	0	0.01568851	0.75277101
		Bingham	0.01769307	0.13787566	0.00347596	1
		HB	0.01580227	0.10278852	0.00574912	0.91558099
	40	Newtonian	0.05882020	0	0.00354718	1
		Ostwald	0.02433985	0	0.01283072	0.76111702
		Bingham	0.01548037	0.11641343	0.00298048	1
		HB	0.01526227	0.10449259	0.00367615	0.96468986
8.5	10	Newtonian	0.33996693	0	0.01204745	1
		Ostwald	0.06310652	0	0.09028608	0.63355101
		Bingham	0.06183610	0.6839501	0.00910274	1
		HB	0.02394891	0.41181163	0.03013344	0.80466496
	20	Newtonian	0.29174205	0	0.00966392	1
		Ostwald	0.06092317	0	0.08158774	0.61174596
		Bingham	0.04756426	0.58890016	0.00712844	1
		HB	0.02490212	0.39780332	0.02129677	0.82117114
	30	Newtonian	0.26507981	0	0.00805042	1
		Ostwald	0.05921402	0	0.08022772	0.58136572
		Bingham	0.03595178	0.5373272	0.00573699	1

		HB	0.02161935	0.4039104	0.01515505	0.84103684
	40	Newtonian	0.23838086	0	0.00682543	1
		Ostwald	0.05074932	0	0.07670339	0.5593563
		Bingham	0.03134528	0.4834777	0.00474384	1
		HB	0.01759544	0.362537	0.01355263	0.82838114
11.2	10	Newtonian	0.78394220	0	0.02280969	1
		Ostwald	0.09020153	0	0.27250713	0.54325247
		Bingham	0.15211880	1.57536001	0.0156115	1
		HB	0.02362131	0.76935175	0.10226952	0.69353407
	20	Newtonian	0.60973351	0	0.0164074	1
		Ostwald	0.09562388	0	0.23246193	0.51157932
		Bingham	0.09203505	1.23471105	0.01076572	1
		HB	0.03577235	0.79531973	0.05241087	0.74072189
	30	Newtonian	0.58554128	0	0.01423216	1
		Ostwald	0.09119943	0	0.25367258	0.46894165
		Bingham	0.07322069	1.19005019	0.00879454	1
		HB	0.02456873	0.83717267	0.04194303	0.74402257
	40	Newtonian	0.53488702	0	0.01225765	1
		Ostwald	0.08359654	0	0.25165824	0.44263891
		Bingham	0.06064463	1.08856316	0.00728375	1
		HB	0.02295327	0.79906866	0.03435327	0.74580198
11.8	10	Newtonian	0.86192863	0	0.02328206	1
		Ostwald	0.09476993	0	0.29523966	0.53730303
		Bingham	0.17130873	1.72827617	0.01584106	1
		HB	0.02711617	0.81330176	0.11408465	0.68144895

	20	Newtonian	0.67732404	0	0.01691761	1
		Ostwald	0.10422007	0	0.25542654	0.50523984
		Bingham	0.10467671	1.36911825	0.01102294	1
		HB	0.04106859	0.86605676	0.05832704	0.72987134
	30	Newtonian	0.64071381	0	0.01472166	1
		Ostwald	0.09338249	0	0.26878597	0.4703402
		Bingham	0.08794704	1.29845637	0.00913122	1
		HB	0.02619350	0.8604639	0.05141247	0.72007678
	40	Newtonian	0.59025856	0	0.01281289	1
		Ostwald	0.08618016	0	0.26755515	0.4456448
		Bingham	0.07259600	1.19846617	0.00765296	1
		HB	0.01901253	0.83611631	0.04237313	0.72273118